AIP | Applied Physics Letters

Effect of direct current sputtering power on the behavior of amorphous indium-gallium-zinc-oxide thin-film transistors under negative bias illumination stress: A combination of experimental analyses and device simulation

Jun Tae Jang, Jozeph Park, Byung Du Ahn, Dong Myong Kim, Sung-Jin Choi, Hyun-Suk Kim, and Dae Hwan Kim

Citation: Applied Physics Letters **106**, 123505 (2015); doi: 10.1063/1.4916550
View online: http://dx.doi.org/10.1063/1.4916550
View Table of Contents: http://scitation.aip.org/content/aip/journal/apl/106/12?ver=pdfcov
Published by the AIP Publishing

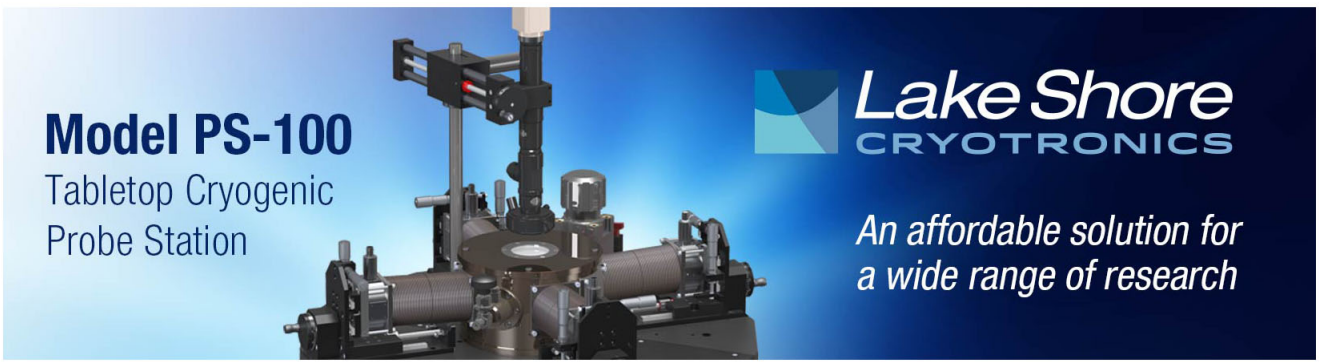

Effect of direct current sputtering power on the behavior of amorphous indium-gallium-zinc-oxide thin-film transistors under negative bias illumination stress: A combination of experimental analyses and device simulation

Jun Tae Jang,[1] Jozeph Park,[2] Byung Du Ahn,[3] Dong Myong Kim,[1] Sung-Jin Choi,[1] Hyun-Suk Kim,[4,a)] and Dae Hwan Kim[1,a)]
[1]*School of Electrical Engineering, Kookmin University, Seoul 136-702, South Korea*
[2]*Department of Materials Science and Engineering, KAIST, Daejeon 305-701, South Korea*
[3]*School of Electrical and Electronic Engineering, Yonsei University, Seodaemun-gu, Seoul 120-749, South Korea*
[4]*Department of Materials Science and Engineering, Chungnam National University, Daejeon 305-764, South Korea*

(Received 8 January 2015; accepted 19 March 2015; published online 26 March 2015)

The effect of direct current sputtering power of indium-gallium-zinc-oxide (IGZO) on the performance and stability of the corresponding thin-film transistor devices was studied. The field effect mobility increases as the IGZO sputter power increases, at the expense of device reliability under negative bias illumination stress (NBIS). Device simulation based on the extracted sub-gap density of states indicates that the field effect mobility is improved as a result of the number of acceptor-like states decreasing. The degradation by NBIS is suggested to be induced by the formation of peroxides in IGZO rather than charge trapping. © *2015 AIP Publishing LLC*.
[http://dx.doi.org/10.1063/1.4916550]

Thin-film transistors (TFTs) incorporating amorphous oxide semiconductors (AOS) have recently attracted a great deal of interest for switching or driving devices in flat panel displays. AOS-TFTs exhibit advantages including high field-effect mobility (μ_{FE}), small subthreshold swing (SS), compatibility with low-temperature process, and optical transparency in the visible range.[1] The most commonly studied material is amorphous indium-gallium-zinc-oxide (a-IGZO),[2] which is already in commercial use in state of the art mobile devices and large-area televisions or monitors.[3]

The current a-IGZO TFTs typically exhibit field effect mobility (μ_{FE}) values near 10 cm^2/V s; however, better performance is required in order to further increase the resolution of large area displays (>100 in.) and allows high frame rate (>240 Hz) operation. An interesting feature about AOS-TFTs is that a trade-off is generally observed between the device performance (for instance, μ_{FE}) and stability under gate bias stress with illumination. Indeed, it has been reported that the reliability of AOS-TFTs with respect to negative-bias-illumination-stress (NBIS) is compromised while one attempts to improve the electrical performance, which is determined by several factors such as the film growth condition and chemical composition of the oxide semiconductor,[4,5] the adjacent passivation layer material and density,[6] and thermal annealing.[7]

Several degradation models have been proposed up to date regarding NBIS: the trapping of photo-generated holes,[8] the photo-desorption of oxygen-related molecules (i.e., interaction with the ambient),[9] the creation of ionized oxygen vacancies,[10] and the formation of metastable O_2^{2-} peroxides.[11] However, relatively few reports provide detailed descriptions on the mechanisms that govern such a trade-off between device performance and stability upon NBIS.

Because the industry requires high throughput, the deposition of oxide semiconductors such as IGZO is usually carried using direct current (DC) sputtering. The latter generally results in growth rates twice as high as those achieved using radio frequency (RF) sputtering. Meanwhile, the deposition conditions must be optimized so as to obtain the best equilibrium between electrical performance and stability of the TFT. In the present work, the effect of DC sputtering power of IGZO is investigated on the resulting TFT performance and stability with respect to NBIS. Quantitative analyses are carried out by the combination of extracted sub-gap density of states (DOS) and device simulation.[12–15] Studies indicate that peroxide formation reflects well the observed behavior of the TFT under NBIS.

IGZO TFT devices with a bottom gate structure were fabricated on glass substrates, including a 50 nm-thick SiO_2 etch stopper layer as shown in Figure 1. The fabrication procedure is described in detail in former publications.[12] 50 nm-thick IGZO layers were grown by DC magnetron sputtering using a single $In_2Ga_2ZnO_7$ target (60 cm × 70 cm), placed at a distance of 6 cm from the substrate. The deposition was done at room temperature in a gas mixing ratio of Ar/O_2 = 35/63 sccm at a fixed total pressure of 5 mTorr. The DC sputtering power was varied from 1 (0.24 W/cm^2) to 3 kW (0.72 W/cm^2). All patterning was done by photolithography and appropriate use of wet or dry etching. The final devices were annealed at 250 °C for 1 h in air. Devices with channel width/length = 25/50 μm were characterized at room temperature using an Agilent 4156C precision semiconductor

a)Authors to whom correspondence should be addressed. Electronic addresses: khs3297@cnu.ac.kr and drlife@kookmin.ac.kr

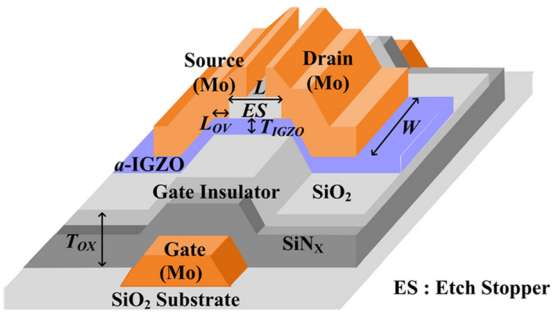

FIG. 1. Schematic illustration of the fabricated a-IGZO TFT.

parameter analyzer. The drain current (I_{DS}) was measured by sweeping the gate-to-source voltage (V_{GS}) from −10 V to 10 V, at a fixed drain-to-source voltage (V_{DS}) of 0.1 V. The NBIS tests were performed for 5000 s with a V_{GS} of −20 V at a fixed V_{DS} of 10 V under illumination with a white light-emitting diode (LED) of 300 cd/m^2 brightness.

The DOS profiles were extracted from the capacitance-voltage (C-V) characteristics of the IGZO TFTs. In detail, the density distribution of acceptor-like sub-gap states, $g_A(E)$, and that of donor-like sub-gap states, $g_D(E)$, were extracted by using the frequency-dependence[13] and photonic response[14] of the C-V characteristics, respectively. The current-voltage (I-V) characteristics were calculated by combining the extracted DOS and a sub-gap DOS-based device simulator (DeAOTS).[15] The electron doping concentration, N_D, was extracted by fitting the measured I-V curves with the calculated ones over a wide range of V_{GS} and V_{DS}.[12,15]

Figure 2(a) shows the representative transfer characteristics of three a-IGZO TFTs, of which the active layers were deposited at DC powers of 1 kW, 2 kW, and 3 kW, respectively. The threshold voltage (V_T) is defined as the V_{GS} value that induces I_{DS} = 10 pA at V_{DS} = 0.1 V. The μ_{FE} was extracted from $g_m/[C_{OX}(W/L)V_{DS}]$ at $(V_{GS} - V_T)/V_{DS}$ = 5/0.1 V, where W is the channel width, L is the channel length, C_{OX} is the gate oxide capacitance per unit area, and g_m is the transconductance defined as $\partial I_{DS}/\partial V_{GS}$. In addition, SS is determined as the minimum value of $\partial V_{GS}/\partial \log(I_{DS})$ in the subthreshold region. The extracted V_T, SS, and μ_{FE} values as a function of the DC sputtering power are shown in Figure 2(b). It is found that higher power results in improved device performance, including high μ_{FE}, small SS, and small V_T values.

Figure 3(a) shows the time evolution of the transfer curves under NBIS, for a-IGZO TFTs fabricated with different IGZO DC sputtering power values. The resulting changes in extracted V_T, μ_{FE}, and SS values with respect to stress time are shown in Figures 3(b)–3(d). All TFTs exhibit parallel negative shifts in V_T without significant variations in μ_{FE} and SS. As the IGZO DC sputter power increases, the devices undergo accelerated degradation upon NBIS. Such results reflect the presence of a trade-off relationship between device performance and reliability.

The DOS-based analyses of the devices were conducted with respect to the IGZO sputter power. The distribution of sub-gap DOS is a very important physical and process-dependent parameter that influences the electrical performance and stability of the TFTs.[16] Figure 4(a) illustrates the DOS model used in this study. It is found that the acceptor-like state distribution, $g_A(E)$, and donor-like state profile, $g_D(E)$, are functions of DC sputter power. The extracted DOS parameters and model equations are summarized in Table I.

The average $g_A(E)$ values near the conduction band minimum (CBM), E_C, decrease with increasing DC power (Figure 4(b)), which accounts well for the enhanced performance of a-IGZO TFTs. This is because a larger amount of acceptor-like sub-gap states near the CBM induces a slow increase of the IGZO Fermi-energy level near the gate insulator interface as the gate voltage is swept from the off state to the on state. This results in larger V_T and SS values. A high DC power is thus expected to provide higher concentrations of free carriers in the conduction band at a fixed gate voltage above the threshold value, which is accompanied with larger μ_{FE} values. Junfei *et al.* indeed reported that a-IGZO films deposited with high sputtering power exhibit high electron concentrations.[17] In addition, note that there is a difference in the saturation behavior between the performance data and extracted $g_A(E)$ values [i.e., from the extracted parameters (Fig. 4(b)), the differences between 1 and 2 kW are smaller than those between 2 and 3 kW conditions. However, in the I-V measurements (Fig. 2), the 2–3 kW differences are much smaller than those between 1 and 2 kW]. Such a result is highly likely to be related to the fact that the parameters describing the TFT performance and stability have a nonlinear and complicated relationship with the DOS values.[18] On the other hand, the total density of donor-like states $g_D(E)$ was divided into donor-like valence band tail

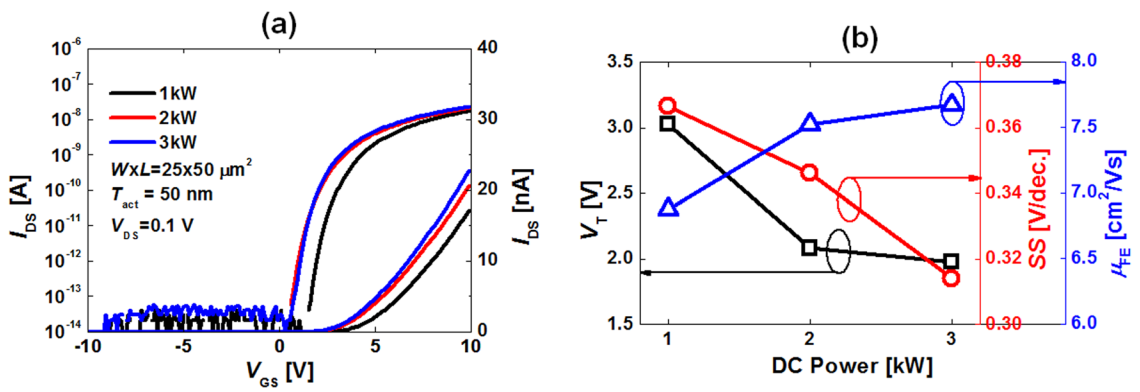

FIG. 2. (a) The measured transfer characteristic at V_{DS} = 0.1 V, (b) V_T, SS, and μ_{FE} with the variation of DC power in a-IGZO TFTs.

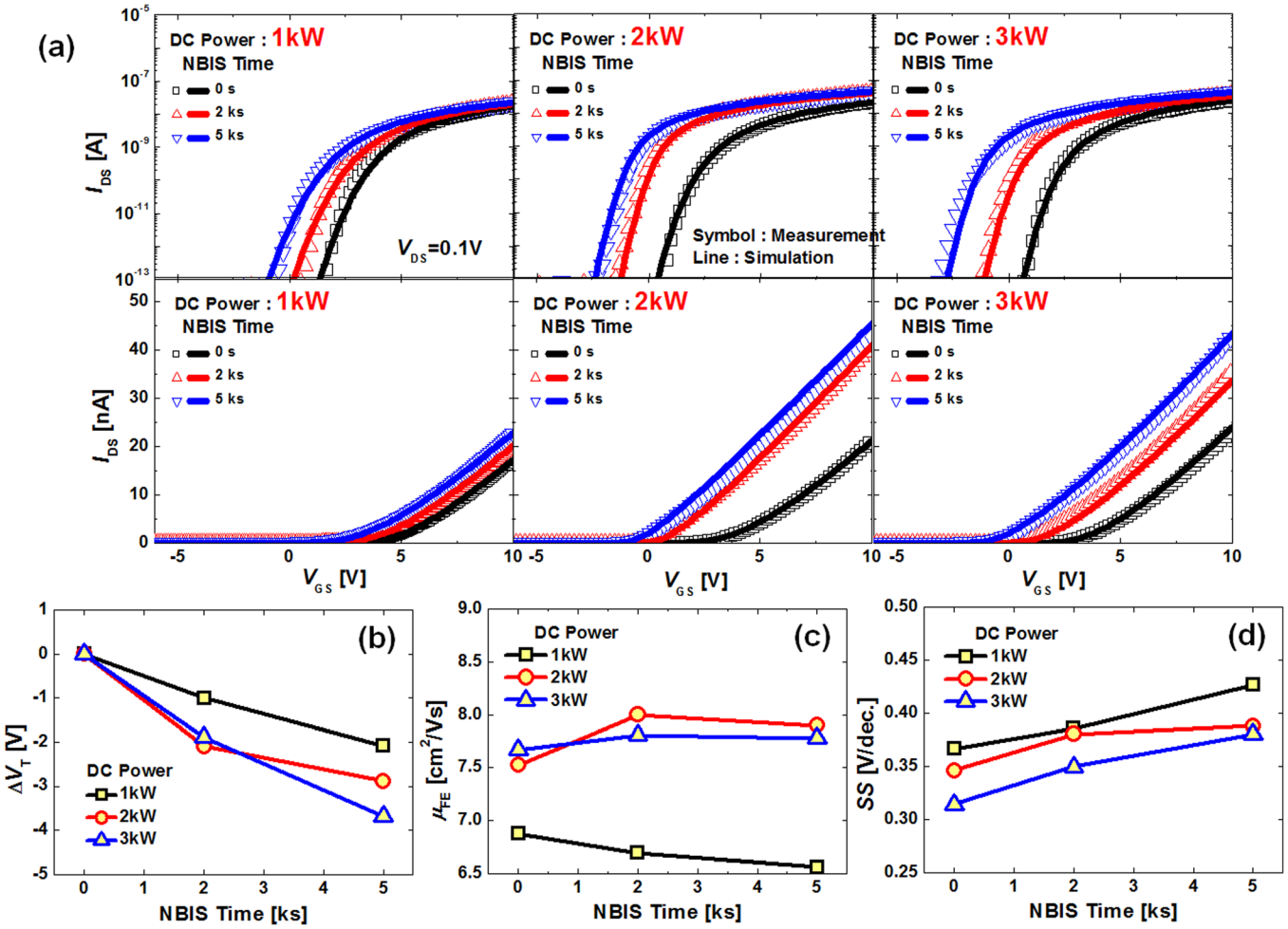

FIG. 3. (a) The measured transfer characteristic at $V_{DS} = 0.1$ V, (b) the change of V_T, ΔV_T, (c) μ_{FE}, and (d) SS during NBIS.

states $g_{TD}(E)$ near the valence band maximum (VBM), E_V, and shallow donor states $g_{SD}(E)$ near the CBM, as shown in Figure 4(c). First of all, as the DC power increases, $g_{TD}(E)$ increases significantly, which may originate from an increase in the structural randomness of amorphous IGZO. Here, it is suggested that the higher sputtering power leads to the formation of stronger local oxygen-oxygen bonds in the IGZO film.[17] The decrease in $g_{SD}(E)$ values is likely to be associated with the suppression of oxygen vacancy ionization because the peak g_{SD} level located at approximately $E_C - 1$ eV is consistent with the position of the V_O^{1+} defect level within the bandgap.[19] Also, it was shown in a former

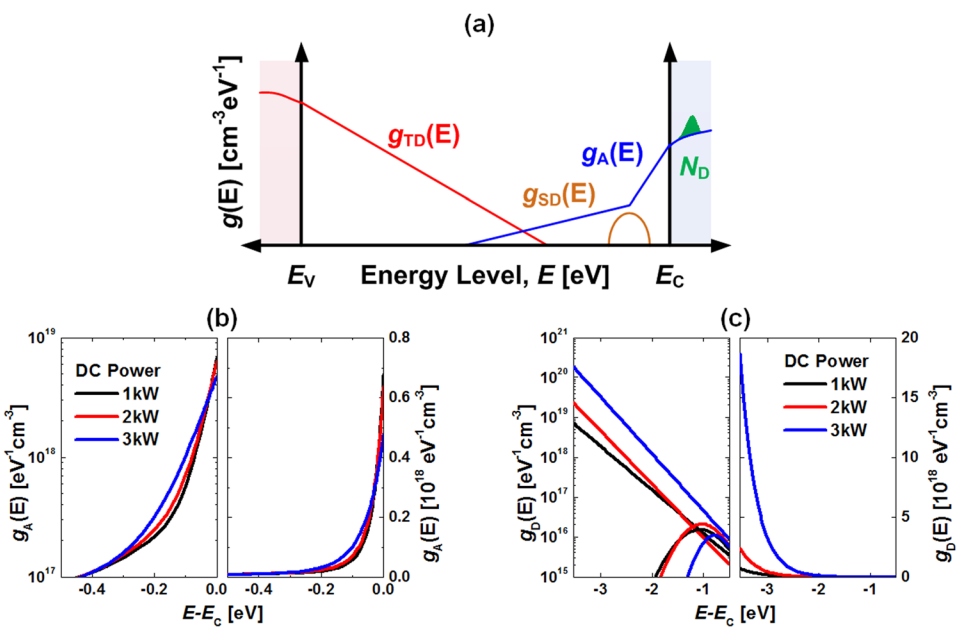

FIG. 4. (a) The used DOS model, (b) extracted $g_A(E)$, and (c) extracted $g_D(E)$ in a-IGZO TFTs before applying the NBIS.

TABLE I. The model and extracted DOS parameters used in the device simulation.

Parameter	Value		
DC power (kW)	1	2	3
E_g (eV)		3.53	
Effective DOS in CBM, N_C (cm^{-3})		1×10^{19}	
Effective DOS in VBM, N_V (cm^{-3})		1×10^{19}	
Doping concentration, N_D (cm^{-3})	2.25×10^{16}	2.18×10^{16}	2.05×10^{16}
Acceptor-like DOS	$g_A(E) = N_{TA} \times \exp\left(\frac{E-E_C}{kT_{TA}}\right) + N_{DA1} \times \exp\left(\frac{E-E_C}{kT_{DA1}}\right) + N_{DA2} \times \exp\left(\frac{E-E_C}{kT_{DA2}}\right)$		
N_{TA}/kT_{TA} ($eV^{-1}\,cm^{-3}$/eV)	$3.78 \times 10^{18}/0.03$	$2.81 \times 10^{18}/0.04$	$2.19 \times 10^{18}/0.06$
N_{DA1}/kT_{DA1} ($eV^{-1}\,cm^{-3}$/eV)	$1.97 \times 10^{17}/0.18$	$2.22 \times 10^{17}/0.13$	…
N_{DA2}/kT_{DA2} ($eV^{-1}\,cm^{-3}$/eV)	$1.41 \times 10^{17}/0.62$	$1.04 \times 10^{17}/0.59$	$0.92 \times 10^{17}/0.70$
Donor-like tail DOS	$g_{TD}(E) = N_{TD} \times \exp\left(\frac{E_V-E}{kT_{TD}}\right)$		
N_{TD}/kT_{TD} ($eV^{-1}\,cm^{-3}$/eV)	$7.23 \times 10^{18}/0.39$	$2.40 \times 10^{19}/0.32$	$1.87 \times 10^{20}/0.30$
Shallow donor DOS	$g_{SD}(E) = N_{D,OV} \times \left(-\left(\frac{E-E_C+E_{D,OV}}{kT_{D,OV}}\right)^2\right)$		
$N_{D,OV}/kT_{D,OV}$ ($eV^{-1}\,cm^{-3}$/eV)	$1.60 \times 10^{16}/0.52$	$2.08 \times 10^{16}/0.46$	$1.07 \times 10^{16}/0.34$
$E_{D,OV}$ (eV)	1.06	1.03	0.78

study that high sputtering power results in the formation of high-density films which may contain reduced concentrations of oxygen vacancies.[20]

The possible physical mechanisms inducing NBIS-degradation were investigated based on the DC power-dependent DOS. First, to examine the trapping of either holes or positively charged ionized oxygen vacancies into the gate insulator and/or at the interface between the gate insulator and the semiconductor, the hole concentration in IGZO near the interface was evaluated under NBIS, as shown in Figure 5(a). As the sputter power increases, the amount of holes accumulating near the interface decreases. The total concentration of trapped holes during NBIS would thus be expected to decrease and result in smaller ΔV_T values. However, this is inconsistent with the experimental results (Figures 3(a) and 3(b)).

The formation of peroxides may be accelerated by the presence of donor-like valence band tail states, $g_{TD}(E)$. In order to look into the possibility of peroxide formation under NBIS, the photo-excited sub-gap energy range (E_C-E_{ph}) ~ E_{Fn} was considered for the ionization of donor-like band-tail states (the dashed region in Figure 5(b)), which is called the

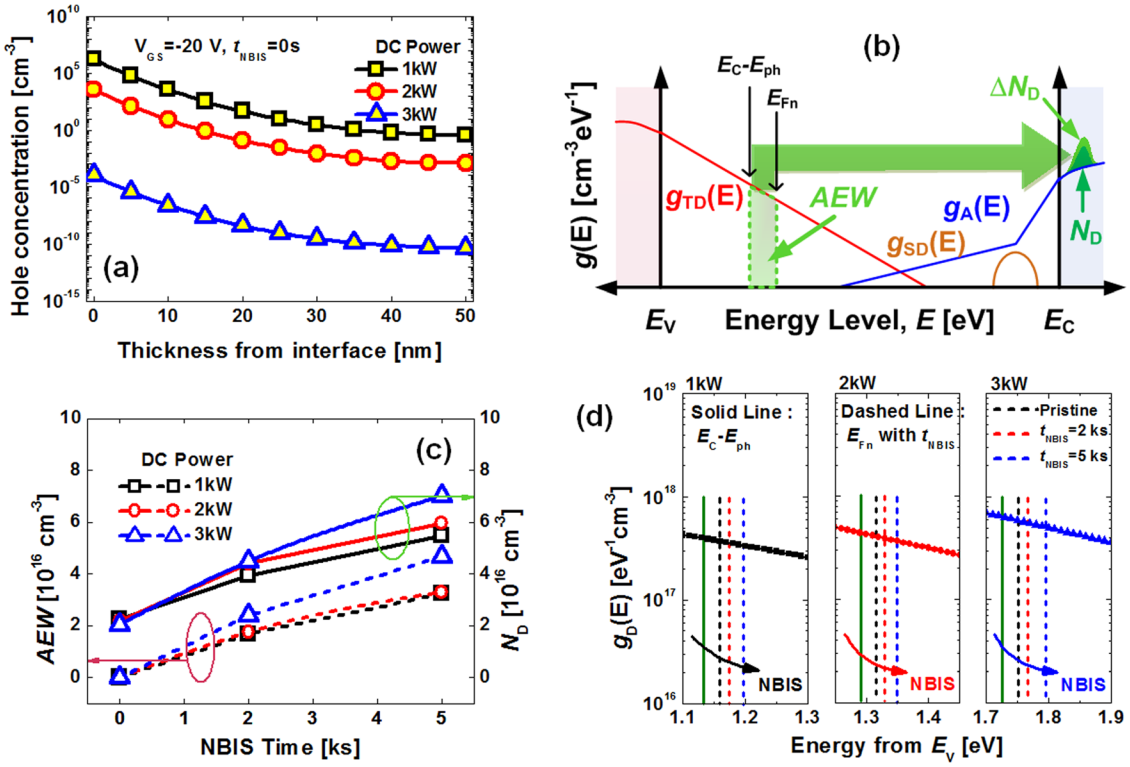

FIG. 5. (a) The calculated hole concentration in a-IGZO TFTs before applying the NBIS, (b) the schematic view of DOS illustrating the transformation of AEW into ΔN_D at a specific time spot during the NBIS, (c) the calculated NBIS time (t_{NBIS}) evolution of AEW and N_D, and (d) the calculated NBIS time evolution of E_{Fn}.

activation energy window (AEW) hereafter. E_{ph} is the effective energy of the incident photons, which is determined by fitting parameters in the DeAOTS simulator (2.40, 2.24, and 1.81 eV for 1, 2, and 3 kW, respectively), and E_{Fn} is the electron quasi-Fermi level. We assume that the photo-excited states do not convert into shallow donor states ($g_{SD}(E)$) by the ionized V_O and that they fully contribute to the incremental donor doping based on the peroxide formation model. The donor creation process may be described as $O^{2-} + O^{2-} \rightarrow O_2^{2-} + 2e^-$. In other words, the AEW at a specific NBIS time $t = t_0$ is described mathematically as

$$\mathrm{AEW}(t = t_0) = \int_{E_c - E_{ph}}^{E_{Fn}(t)} g_{TD}(E)dE|_{t=t_0} \quad (1)$$

and is identical to the increment of electron doping concentration N_D between adjacent time spots $t = t_0$ and $t = t_0 + \Delta t$, i.e., $\mathrm{AEW}(t_0) = \Delta N_D(t = t_0 + \Delta t) = N_D(t = t_0 + \Delta t) - N_D(t = t_0)$. Figure 5(c) shows the time evolution of $\mathrm{AEW}(t)$ and $N_D(t)$ with respect to NBIS, depending on the DC power. Here, the $\mathrm{AEW}(t=0)$ was calculated from the DOS and N_D, which were extracted before the NBIS experiment. The quasi Fermi level, $E_{Fn}(t=t_0)$, which is a required parameter to estimate $\mathrm{AEW}(t_0)$, was determined by device simulation using the aforementioned DOS and $N_D(t=t_0)$ as parameters. It is suggested that the AEW increases due to the increasing $E_{Fn}(t)$ level with increasing DC power (Figure 5(d)). As a result, the DOS-based calculations, indicated by solid lines in Figure 3(a), correlate well with the measured transfer curves (symbols in Figure 3(a)), suggesting that both the extracted DOS and the calculated time evolution of N_D (Figure 5(c)) are reasonable. Therefore, a simple increase of electron doping concentration without any change of SS or sub-gap state distribution may be explained by the peroxide O_2^{2-} formation rather than by the trapping of positive charge.

In conclusion, the effect of DC sputter power during IGZO growth on the performance and reliability of the resulting TFTs was quantitatively analyzed by combining the experimentally extracted DOS and device simulation. The extracted acceptor-like DOS distribution, $g_A(E)$, decreases as the DC power increases, which has a significant influence on the enhancement of field effect mobility, with less positive V_T and small SS values. On the other hand, the extracted density of donor-like valence band tail states, $g_{TD}(E)$, increases with increasing DC power. Based on the extracted $g_{TD}(E)$, the degradation of the TFT devices under NBIS is well explained by the donor creation model based on peroxide formation without ionized oxygen vacancies. The methodology presented in this work provides a physical insight on the trade-off between device performance and reliability of AOS TFTs.

This work was supported by BK21+ with the Educational Research Team for Creative Engineers on Material-Device-Circuit Co-Design (Grant No. 22A20130000042), National Research Foundation of Korea through the Ministry of Education, Science and Technology under (Grant No. 2014-025176), and IC Design Education Center (IDEC). This work was also supported by research fund of Chungnam National University.

[1]E. Fortunato, P. Barquinha, and R. Martins, Adv. Mater. **24**, 2945 (2012).
[2]T. Kamiya, K. Nomura, and H. Hosono, Sci. Technol. Adv. Mater. **11**, 044305 (2010).
[3]W.-J. Nam, J.-S. Shim, H.-J. Shin, J.-M. Kim, W.-S. Ha, K.-H. Park, H.-G. Kim, B.-S. Kim, C.-H. Oh, B.-C. Ahn, B.-C. Kim, and S.-Y. Cha, SID Int. Symp. Digest Tech. Papers **44**, 243–246 (2013).
[4]H.-S. Kim, K.-B. Park, K. S. Son, J. S. Park, W.-J. Maeng, T. S. Kim, K.-H. Lee, E. S. Kim, J. Lee, J. Suh, J.-B. Seon, M. K. Ryu, S. Y. Lee, K. Lee, and S. Im, Appl. Phys. Lett. **97**, 102103 (2010).
[5]H.-S. Kim, J. S. Park, W.-J. Maeng, K. S. Son, T. S. Kim, M. Ryu, J. Lee, J. C. Lee, G. Ko, S. Im, and S. Y. Lee, IEEE Electron Device Lett. **32**, 1251 (2011).
[6]J. S. Park, T. S. Kim, K. S. Son, K.-H. Lee, W.-J. Maeng, H.-S. Kim, E. S. Kim, K.-B. Park, J.-B. Seon, W. Choi, M. K. Ryu, and S. Y. Lee, Appl. Phys. Lett. **96**, 262109 (2010).
[7]S. Kim, Y. Jeon, J.-H. Lee, B. D. Ahn, S. Y. Park, J.-H. Park, J. H. Kim, J. Park, D. M. Kim, and D. H. Kim, IEEE Electron Device Lett. **31**, 1236 (2010).
[8]J.-Y. Kwon, J. S. Jung, K. S. Son, K.-H. Lee, J. S. Park, T. S. Kim, J.-S. Park, R. Choi, J. K. Jeong, B. Koo, and S. Y. Lee, Appl. Phys. Lett. **97**, 183503 (2010).
[9]J. K. Jeong, H. W. Yang, J. H. Jeong, Y.-G. Mo, and H. D. Kim, Appl. Phys. Lett. **93**, 123508 (2008).
[10]A. Janotti and C. G. Van deWalle, Phys. Rev. B **76**, 165202 (2007).
[11]H.-H. Nahm, Y.-S. Kim, and D. H. Kim, Phys. Status Solidi B **249**, 1277 (2012).
[12]Y. Kim, M. Bae, W. Kim, D. Kong, H. K. Jeong, H. Kim, S. Choi, D. M. Kim, and D. H. Kim, IEEE Trans. Electron Device **59**, 2689 (2012).
[13]S. Lee, S. Park, S. Kim, Y. Jeon, K. Jeon, J.-H. Park, J. Park, I. Song, C. J. Kim, Y. Park, D. M. Kim, and D. H. Kim, IEEE Electron Device Lett. **31**, 231 (2010).
[14]H. Bae, H. Choi, S. Jun, C. Jo, Y. H. Kim, J. S. Hwang, J. Ahn, S. Oh, J.-U. Bae, S.-J. Choi, D. H. Kim, and D. M. Kim, IEEE Electron Device Lett. **34**, 1524 (2013).
[15]Y. W. Jeon, S. Kim, S. Lee, D. M. Kim, D. H. Kim, J. Park, C. J. Kim, I. Song, Y. Park, U.-I. Chung, J.-H. Lee, B. D. Ahn, S. Y. Park, J.-H. Park, and J. H. Kim, IEEE Trans. Electron Device **57**, 2988 (2010).
[16]Y. Kim, S. Kim, W. Kim, M. Bae, H. K. Jeong, D. Kong, S. Choi, D. M. Kim, and D. H. Kim, IEEE Trans. Electron Device **59**, 2699 (2012).
[17]S. Junfei, D. Chengyuan, D. Wenjun, W. Jie, C. Yuting, and Z. Runze, J. Semicond. **34**, 084003 (2013).
[18]M. Bae, K. M. Lee, E.-S. Cho, H.-I. Kwon, D. M. Kim, and D. H. Kim, IEEE Trans. Electron Device **60**, 3465 (2013).
[19]P. Migliorato, M. D. H. Chowdhury, J. G. Um, M. Seok, and J. Jang, Appl. Phys, Lett. **101**, 123502 (2012).
[20]B. S. Yang, S. Oh, Y. J. Kim, S. J. Han, H. W. Lee, H. J. Kim, H. K. Park, J. K. Jeong, J. Heo, C. S. Hwang, and H. J. Kim, J. Vac. Sci. Technol., B **32**, 011202 (2014).